



HHS Public Access

Author manuscript

Abdom Radiol (NY). Author manuscript; available in PMC 2018 December 03.

Published in final edited form as:

Abdom Radiol (NY). 2018 November ; 43(11): 3166–3175. doi:10.1007/s00261-018-1581-5.

Contrast-enhanced ultrasonography in interventional oncology

Sriharsha Gummadi^{1,2}, John R. Eisenbrey², and Andrej Lyshchik²

¹Department of Surgery, Lankenau Medical Center, Wynnewood, PA, USA

²Department of Radiology, Thomas Jefferson University, Philadelphia, PA, USA

Abstract

Contrast-enhanced ultrasound (CEUS) has evolved from the use of agitated saline to second generation bioengineered microbubbles designed to withstand insonation with limited destruction. While only one of these newer agents is approved by the Food and Drug Administration for use outside echocardiography, interventional radiologists are increasingly finding off-label uses for ultrasound contrast agents. Notably, these agents have an extremely benign safety profile with no hepatic or renal toxicities and no radiation exposure. Alongside diagnostic applications, CEUS has begun to develop its own niche within the realm of interventional oncology. Certainly, the characterization of focal solid organ lesions (such as hepatic and renal lesions) by CEUS has been an important development. However, interventional oncologists are finding that the dynamic and real-time information afforded by CEUS can improve biopsy guidance, ablation therapy, and provide early evidence of tumor viability after locoregional therapy. Even more novel uses of CEUS include lymph node mapping and sentinel lymph node localization. Critical areas of research still exist. The purpose of this article is to provide a narrative review of the emerging roles of CEUS in interventional oncology.

Keywords

Contrast-enhanced ultrasound; Interventional oncology; Interventional radiology

Since the 1960s with early use of agitated saline for cardiac and vascular ultrasound enhancement, the field of contrast-enhanced ultrasonography (CEUS) has grown tremendously [1]. CEUS has found diagnostic applications in echocardiography, solid organ investigation, vascular morphology, and extravascular interrogation (lymphatic, biliary, intracavitary) [2]. Established clinical guidelines exist in echocardiography and hepatic ultrasound with emerging literature advocating for guidelines in other diagnostic applications including renal and thyroid ultrasound [2, 3].

Correspondence to: Andrej Lyshchik; Andrej.Lyshchik@jefferson.edu.

Conflicts of interest The authors report non-financial and grant support from GE Healthcare and Toshiba Medical Systems outside the submitted work.

Ethical approval All procedures performed in studies involving human participants were in accordance with the ethical standards of the institutional and/or national research committee and with the 1964 Helsinki declaration and its later amendments or comparable ethical standards. Because all clinical vignettes contain only de-identified retrospective data and are utilized for educational purposes only, no consent outside standard procedural consent was requested of any patients.

Contrast-enhanced ultrasound relies on the inherent non-linear scatter of microbubble-based ultrasound contrast agents (UCA) [4]. Because tissues generally produce linear scatter at the transmit frequency f_0 , pulse inversion or other non-linear-based software can be used to suppress the surrounding tissue [4]. By detecting scatter at the harmonic ($2 \times f_0$), subharmonic ($0.5 \times f_0$) or superharmonic ($n \times f_0$) levels, greater contrast-to-tissue signal ratio can be achieved [4].

Real-time ultrasonography, cross-sectional imaging, and digital subtraction angiography/fluoroscopy are key tools in an interventional radiologist's arsenal. With an emergence of CEUS in diagnostic applications, the natural evolution of the technology is towards interventional practices [2]. The oncologic applications of CEUS are readily apparent as solid tumor malignancies can be defined by characteristic enhancement patterns and treatment response by changes in vascularity [3]. The purpose of this review is to highlight the various emerging roles of CEUS in interventional oncology.

Ultrasound contrast agents

A variety of UCA are now commercially available [1]. These agents are characterized by an outer stabilizing shell and inner gas core. Because of their size (1–6 μM , approximating the size of a red blood cell), these microbubbles are too large to extravasate from the blood stream into the interstitium [5]. This blood pooling characteristic makes these agents ideal for vascular and delayed vascular imaging. [5] The improved signal-to-noise ratio affords for improved lesion characterization. [1] First generation UCA used an air gas core [1]. These microbubbles were very fragile and short-lived because of the high solubility of air in blood [1]. Second generation UCA contain a high molecular weight, low blood solubility gas core [1]. Biomaterials engineered to serve as a stabilizing outer shell include phospholipids, surfactants, polymers, and proteins [1]. These newer generation UCA are more stable and can be imaged in real-time with less risk of unintended bubble destruction [1]. The microbubbles are excreted through the lungs as inert exhaled gas [6]. Remnant phospholipid shells are hydrolyzed to free fatty acids [6].

UCA have a remarkably benign safety profile [4]. They may be safely used in patients with renal or hepatic impairment with no concern for nephrotoxicity [4]. There is no radiation exposure [4]. Reported side effects are relatively mild and include headache, dizziness, nausea, back pain, flushing, chest pain, and rarely allergic reaction [4].

In the United States, three second generation contrast agents are approved by the Food and Drug Administration (FDA) for echocardiography: Optison (GE Healthcare, Princeton, NJ), Definity (Lantheus Medical Imaging, N. Billerica, MA), and Lumason (Bracco Diagnostics, Monroe Township, NJ) [7]. While only Lumason is FDA approved for hepatic ultrasonography (as of 2016), Definity is also regularly used off-label for hepatic contrast studies [8]. Methods of reimbursement for off-label CEUS have been addressed and are dependent on the clinical setting [9]. A fourth agent, Sonazoid (GE Healthcare, Oslo, Norway) is not FDA approved for any indication within the United States but is approved for use in South Korea, Norway, and Japan for focal hepatic lesion characterization [10]. Additionally, Sonazoid is approved in Japan for characterization of focal breast lesions [11].

This agent may also be uniquely positioned for the characterization of liver lesions, lymphatics, and lymph nodes due to uptake by the reticuloendothelial system [2, 10]. Specifically, Sonazoid is taken up by Kupffer cells within normal liver [3]. This results in a “Kupffer-phase” pattern of enhancement (10 min after injection) in normal liver that is not appreciated in hepatic adenoma or hepatocellular carcinoma (HCC) [3].

Technical considerations

Adequate CEUS examination necessitates many of the same principals as standard ultrasound including patient positioning, probe selection, and careful attention to focal point and gain. However, additional considerations exist. Appropriate patient and technique selection per interventional procedure is paramount.

CEUS is best situated for targeted assessments rather than general examinations because of the need to examine entire contrast kinetics of the target. This can make select situations difficult—such as the cirrhotic liver where identification of specific nodules of concern by gray-scale may be difficult and obscured by a coarse heterogeneous hepatic window [12]. Additionally, because commercially available CEUS rely on superharmonics, penetration and imaging of deeper structures may be limited. CEUS is “operator-dependent”—even more so than conventional ultrasound. In our practice, the radiologist accompanies the sonographer during the examination and requires active participation [13]. This is unlike CT or MRI and can be an obstacle to adoption in many institutions [13].

Low mechanical index (MI) sonography should be utilized (< 0.3) to avoid bubble cavitation/destruction. This is important because we recommend performing CEUS in split-screen mode with gray-scale display alongside CEUS images for improved anatomic localization. Standard gray-scale sonography will destroy many of the bubbles without attention to manufacturer set MI. Like color and power Doppler, time-elapsed clips should be recorded through each phase of every lesion in question—the strength of CEUS is its ability to provide dynamic information.

Intravenous (IV) access is required for CEUS. We recommend at least a 20-gauge catheter to avoid inadvertent bubble destruction during administration. Generally, we recommend bolus dose administration (refer to package insert for maximum dose) followed by 5–10 mL normal saline flush for most applications. However, if quantitative enhancement analysis or extended examination is desired, an infusion may be utilized to provide consistent vascular opacification. Increasing the bolus dose should typically be avoided, particularly in deeper lesions, because this limits penetration. If re-examination is required, repeat injection may be performed (with attention to maximum dose per manufacturer guidelines) after existing microbubbles have been eliminated. This may take at least 5–10 min.

Focal lesion characterization

CEUS has shown to be a valuable decision-making adjunct to standard cross-sectional imaging in the diagnosis of focal solid organ tumors including liver and renal lesions. CEUS provides real-time imaging and parenchymal enhancement allowing for a stronger temporal understanding of lesion vascularity dynamics [2]. Additionally, because of their benign

safety profile of UCA, examination may be repeated in cases of study inadequacy up to a maximum allowable dose per the agent [3]. For the interventional oncologist, CEUS is particularly salient in diagnostic dilemmas regarding focal hepatic and renal lesions, especially in patients with contrast-enhanced magnetic resonance imaging (MRI) or computed tomography (CT) contraindications such as low glomerular filtration rate (GFR), pacemakers, or claustrophobia [2, 3].

Focal liver lesions

On CEUS, focal liver lesions can be characterized by the timing and pattern of enhancement at each of three phases of examination timed from the beginning of the infusion of contrast: arterial (10–45 s), portal (45–120 s), and late venous (120 s to bubble disappearance) [3]. This is similar to contrast-enhanced CT or MRI of focal liver lesions. These are summarized in Table 1. Specifically, benign lesions tend to maintain enhancement through portal and late venous phases (with the exception of simple cysts which do not enhance in any phase) [3]. They can be differentiated by their patterns of enhancement [3]. Contrastingly, malignant lesions are characterized by variable arterial enhancement with notable portal and late venous phase washout [3]. In 2017, The American College of Radiology (ACR) has published a CEUS LI-RADS system to standardize the diagnosis of HCC using CEUS based on these characteristics [14].

Clinical vignette: focal liver lesion

A contrast-enhanced CT scan performed of a 33-year-old female revealed an indeterminate hypodense 1.2-cm lesion in the left hepatic lobe. The patient was initially referred for ultrasound-guided biopsy of the lesion. After discussion with the referring team, CEUS of the liver lesion was first performed. The examination was performed using a bolus dose 0.2 mL Definity (N. Billerica, MA) as UCA. The examination revealed a $1.4 \times 1.3 \times 1.6$ cm lesion with peripheral discontinuous globular enhancement (extending from the left of image towards the center of the lesion) in the arterial phase and no washout (Fig. 1). The lesion was determined to be a hemangioma and biopsy was avoided.

Focal renal lesions

Similarly, CEUS has been shown to be valuable in the characterization of indeterminate renal lesions. Solid renal masses with enhancement and early washout are highly suggestive of malignancy (in the absence of macroscopic adipose tissue) [4,15]. Additionally, enhancement of renal vein thrombus can suggest tumor thrombus (as opposed to bland thrombus) [2]. In cystic renal masses, CEUS features suggestive of malignancy include the presence of nodular/thick enhancing septations and heterogeneous patchy lesion enhancement [15]. Contrastingly, lack of enhancement or the presence of very thin poorly enhancing septations suggests against malignancy [15]. Supportive studies are currently being performed for the creation of a standardized system of diagnosis for renal cell carcinoma with a particular emphasis on the role of CEUS [15, 16].

Clinical vignette: focal renal lesion

On non-contrast CT scan, an incidental $7.4 \times 4.2 \times 8.6$ cm exophytic renal mass was detected in an 88-year-old male with chronic kidney disease (Fig. 2A). CT contrast agent was contraindicated due to patient's poor GFR. Instead, CEUS was performed using bolus dose 0.2 mL Definity (N. Billerica, MA) as UCA. The examination revealed $7.1 \times 7.0 \times 6.2$ complex cystic lesion with no internal enhancement, consistent with a benign hemorrhagic or proteinaceous cyst (Fig. 2C). Biopsy was avoided, and the patient was recommended for interval follow-up.

Image guidance for interventional procedures

CEUS can be useful in providing real-time procedural imaging guidance. Discrimination of viable, actively perfused areas of tumor from necrotic/cystic areas can be used to overcome biopsy-associated sampling error [2]. Additionally, immediate tumor perfusion analysis allows for real-time responsive feedback to thermal ablative therapies [17, 18]. The role of CEUS in lymph node interrogation is currently evolving with applications in sentinel and staging lymph node assessments [19].

Image guidance for percutaneous procedures

As stated, CEUS has shown the ability to improve image-guided percutaneous biopsies in a variety of solid organs. CEUS provides real-time perfusion imaging allowing for the interventional radiologist to more accurately target the actual pathology of the lesion rather than a cystic pocket or the necrotic core [2]. Utilizing CEUS, liver biopsy diagnostic accuracy in tumors can rise from as low as 87% to as high as 96%–100% [20, 21]. Additionally, CEUS has been used to guide biopsies in liver lesions not visible on gray-scale ultrasound [22]. CEUS has also shown value in renal and lung tumors [2, 23–25]. However, application to solid organ biopsy guidance is still in its infancy. Early comparative results are summarized in Table 2. While early series have not shown any improvement in diagnostic accuracy or sensitivity with the use of CEUS in endoscopic ultrasound (EUS)-guided fine needle aspiration (FNA) for pancreatic lesions, Sugimoto et al. 2015 described increased interventional efficiency with the use of CEUS-EUS-FNA compared with EUS-FNA (by percent of samples demonstrating sufficiency with a single needle pass, 60% vs. 25%, $N=20$ vs. 20, $P < 0.05$) [26].

Newer is CEUS to guide targeted prostate biopsies for prostate adenocarcinoma [2]. Because transrectal ultrasonography using gray-scale or power doppler ultrasound has shown to be poor predictors for identifying malignancy, interventional radiologists and urologists must perform thorough and systematic multi-core prostate biopsies of all regions [2, 27]. However, because of the increased micro-vascularity found in prostate cancer, nodular enhancement seen on CEUS may serve as a valuable guide [2, 28–30]. Centers are now performing randomized controlled trials assessing this potential for increasing relevant tissue sampling [28]. The performance of CEUS-guided biopsy compared with the multi-core systematic technique shows variable significance. Halpern et al. 2012 even reports increased detection rate of the multi-core systematic technique (39% vs. 26%, $P < 0.001$) [28]. However, after performing analysis per-core retrieved (rather than per patient examined),

CEUS-guided biopsy appears to nearly ubiquitously demonstrate increased diagnostic yield (see Table 3). This suggests that routine detection rate may, in part, be supplemented simply by increased sampling [31]. Still, CEUS-guided biopsy in prostate cancer shows poor overall yields due to inadequate suppression of normal tissue enhancement or vascularity [28].

Attempts at chemical (such as 5 α -reductase inhibitors) and technical (including subharmonic imaging, elastography, and multi-parametric or fusion imaging) discrimination from benign prostate tissue are currently at the forefront [28, 32].

Clinical vignette: CEUS-assisted percutaneous biopsy

A contrast-enhanced CT demonstrated an enlarging 8 \times 4 \times 5 cm heterogeneously enhancing left flank mass in a 65-year-old male with a known history of melanoma (Fig. 3A). Multiple ultrasound and CT-guided guided core needle biopsies of this lesion were performed at an outside institution, all showing only necrotic debris on pathology. Consequently, a CEUS-guided 18-gauge core needle biopsy was performed using a bolus dose 0.5 mL Definity (N. Billerica, MA) as UCA. The bolus dose was administered twice—first to delineate the lesion and a second time for real-time needle guidance. The enhancing portion of the lesion was targeted (Fig. 3C) to avoid necrotic elements of the mass. Pathology was consistent with metastatic melanoma and the patient was referred to the oncology service for further management.

Image guidance for thermal ablation therapies

Similarly, interventional oncologists can utilize CEUS for image guidance during thermal ablation because of its ability to delineate real-time tumor perfusion dynamics [33]. Pre-procedural CEUS allows for high fidelity treatment margin identification and the development of an precise volumetric map [2]. Additionally, intra-procedural CEUS can allow for accurate targeting for ablation [2]. Electrode placement during percutaneous thermo-ablative therapy can be difficult in lesions that are incompletely visualized on gray-scale sonography [34]. In patients with HCC poorly imaged by grayscale ultrasound selected for radiofrequency ablation, Minami et al. 2004 demonstrated complete tumor necrosis with a single session of treatment in 95.2% of the patients treated by CEUS guidance versus 32% in patients treated by gray-scale ultrasound guidance alone ($N=21$ vs. 25) [35]. Finally, CEUS has shown immediate value in assessment of incomplete treatment (performed while the patient is still in the interventional suite)—with a reduction in up to 31% of patients requiring a second treatment [17, 18].

Evaluation of lymph nodes

CEUS still appears to be limited (as gray-scale ultrasound) in differentiating malignant from benign lymph nodes [2]. On CEUS, tumor-involved lymph nodes may show a filling defect representing rarefaction of nodal vessels by tumor invasion, but this finding is not invariable [36]. However, UCA injected peri-tumorally have been shown to distribute along adjacent lymphatics in a fashion similar to standard blue dye and tracer methods for the identification of sentinel nodes [19]. Compared with the blue dye and tracer methods, CEUS allows for real-time tracking without the need for surgical dissection. CEUS-assisted preoperative wire localization of sentinel lymph nodes has been described [37]. This has value in the

prognostication and treatment of cutaneous melanoma and breast cancer. However, this application is still largely experimental.

Early assessment of tumor response after locoregional treatment

Contrast-enhanced cross-sectional imaging is the traditional method of assessing tumor response after locoregional treatment of solid organ tumors. However, in addition to being cumbersome and limited intra-operatively (such as with cone beam CT), imaging is frequently delayed from between 1 week to up to several months after therapy to reduce obscuration of nodular peripheral tumor viability or recurrence by reactive hyperemia (and to reduce lipiodol artifact if CT is pursued). [38–40] This limits the potential for early intervention in patients harboring residual viable malignancy. CEUS may help to identify these early treatment failures and serve as an adjunct assessment in patients with contraindications to MRI or CT contrast (such as renal insufficiency) after locoregional therapy.

Tumor response: hypothermal ablative therapy

Hypothermal ablative therapy (cryoablation) mediates cellular destruction by repeated freeze–thaw–refreeze cycles induced by a needle-sized cryoprobe [41]. When utilized for renal cell carcinoma, contrast-enhanced CT may be delayed as late as 4 months after treatment to reduce false positives from post-ablation inflammation [4]. Following confirmation of effective therapy, variable surveillance protocols exist. However, many of these patients suffer from low GFR, and thus gadolinium and iodinated contrast are contraindicated. First described in 2005, early experience with CEUS in cryoablation suggests excellent concordance (with up to 100% sensitivity and between 90% and 100% specificity) with contrast-enhanced cross-sectional imaging without renal toxicity or radiation [42–45]. However, admittedly, available data for CEUS after cryoablation are still currently extremely limited and comprised primarily of case series and limited sample sizes.

Clinical vignette: monitoring treatment effect after cryoablation

CT scan performed of a 74-year-old male revealed a 3.4-cm right renal lesion with enhancement concerning for renal cell carcinoma (Fig. 4A). Due to the patient's medical comorbidities, the patient was deemed a poor surgical candidate and percutaneous cryotherapy was instead performed. A CEUS examination was performed 8 months later showing a post-ablation cavity without any nodular enhancing component, suggesting complete response to therapy (Fig. 4C).

Tumor response: hyperthermal ablative therapy

Hyperthermal ablative therapies (such as microwave ablation) rely on heat produced by resistive tissue friction by needle-sized radiofrequency probes to cause cellular destruction (and protein denaturation or even cellular vaporization) [41]. As noted earlier, CEUS has been used for immediate assessment of treatment effect to reduce the rates of incomplete radiofrequency ablation for HCC to as low as 6% after initial treatment [3, 46]. This has the potential of reducing the healthcare costs associated with retreatment [17]. Table 4 summarizes our current understanding regarding the performance of CEUS in treatment-

monitoring after cryoablative and hyperthermal ablative therapies in renal and hepatic lesions. Early CEUS (performed within 24-h post-treatment) may have limited sensitivity to inadequate treatment (as low as 40%) due to difficulty in differentiating viable tumor from post-procedural reactive hyperemia and technical limitations (such as poor patient tolerance post-anesthesia and interposed bowel gas) [47–50]. However, specificities between 98% and 100% suggest that early CEUS may still play a role in post-procedural survey. [47–49] Importantly, CEUS obtained at least one month after therapy has shown to be concordant with contrast-enhanced cross-sectional imaging with sensitivities between 79% and 100% and specificities between 92.9% and 100% [43, 49].

Tumor response: intra-arterial embolization therapy

Finally, intra-arterial embolization therapies such as trans-arterial chemoembolization (TACE) and trans-arterial radioembolization (TARE) have found a particular role in locally advanced HCC and as a bridge to hepatic transplantation [41]. As in thermal ablative therapies, cross-sectional imaging is obtained only after 4 weeks after therapy to minimize artifacts associated with inflammatory hyperemia and lipiodol (the latter for if CT is performed) [38, 39]. However, early findings suggest that CEUS can detect residual tumor viability and enhancement in as little as one week following treatment with strong concordance [39]. Notably, the literature is limited with regard to direct comparative studies evaluating CEUS verse contrast-enhanced cross-sectional imaging in patients with TACE. The literature is even sparser with regard to TARE. Table 5 summarizes the salient studies illustrating the performance of CEUS after TACE in HCC.

Clinical vignette: monitoring treatment effect after TACE

A CT scan obtained of a 65-year-old male with HCC shows a $2.8 \times 2.6 \times 2.5$ cm segment VI lesion (LIRADS 5) with arterial enhancement (Fig. 5A) and brisk washout on delayed imaging. The patient underwent TACE with drug-eluting beads containing doxorubicin via the segment 6 branch of the right hepatic artery. CEUS performed one week after TACE shows partial tumor response with a small portion of the lesion still enhancing, favoring residual viable tumor (Fig. 5C). This was later confirmed on follow-up MRI.

Conclusion

CEUS has gained significant momentum since its inception in the 1960s. CEUS is well positioned as a problemsolving tool for an interventional radiologist's diagnostic dilemmas. Newest applications include lesion targeting and treatment effect monitoring. Significant impetus exists for further clinical research and engineering innovation as novel roles continue to mature within interventional oncology.

Acknowledgments

Funding Research reported in this publication was supported by the National Institutes of Health under the award numbers R01CA194307 and R01CA215520. The content is solely the responsibility of the authors and does not necessarily represent the official views of the National Institutes of Health.

References

1. Paefgen V, Doleschel D, Kiessling F (2015) Evolution of contrast agents for ultrasound imaging and ultrasound-mediated drug delivery. *Front Pharmacol* 6:197 [PubMed: 26441654]
2. Piscaglia F, Nolsøe C, Dietrich CF, et al. (2012) The EFSUMB guidelines and recommendations on the clinical practice of contrast enhanced ultrasound (CEUS): update 2011 on non-hepatic applications. *Ultraschall in der Medizin-Eur J Ultrasound* 33(01):33–59
3. Claudon M, Dietrich CF, Choi BI, et al. (2013) Guidelines and good clinical practice recommendations for contrast enhanced ultrasound (CEUS) in the liver—update 2012. *Ultraschall in der Medizin-Eur J Ultrasound* 34(01):11–29
4. Eisenbrey JR, Sridharan A, Liu J- B, et al. (2015) Recent experiences and advances in contrast-enhanced subharmonic ultrasound. *BioMed Res Int* 2015:1–6
5. Eisenbrey JR, Wilson CC, Ro RJ, et al. (2013) Correlation of ultrasound contrast agent derived blood flow parameters with immunohistochemical angiogenesis markers in murine xenograft tumor models. *Ultrasonics* 53(7):1384–1391 [PubMed: 23659876]
6. Definity R [Package Insert] (2017) Lantheus Medical Imaging, North Billerica, MA, http://www.definityimaging.com/pdf/DEFINITY_US_PL_515987-0117.pdf. Accessed 6 Nov 2017
7. Muskula PR, Main ML (2017) Safety with echocardiographic contrast agents. *Circulation* 10(4):e005459 [PubMed: 28377467]
8. Lyshchik A, Kono Y, Dietrich CF, et al. (2017) Contrast-enhanced ultrasound of the liver: technical and lexicon recommendations from the ACR CEUS LI-RADS working group. *Abdom Radiol* 38:1–19
9. Barr RG (2013) Off-label use of ultrasound contrast agents for abdominal imaging in the United States. *J Ultrasound Med* 32(1):7–12 [PubMed: 23269705]
10. Forsberg F, Piccoli CW, Liu J- B, et al. (2002) Hepatic tumor detection: MR imaging and conventional US versus pulse-inversion harmonic US of NC100100 during its reticuloendothelial system-specific phase. *Radiology* 222(3):824–829 [PubMed: 11867808]
11. Li P, Hoppmann S, Du P, et al. (2017) Pharmacokinetics of Perfluorobutane after Intra-Venous Bolus Injection of Sonazoid in Healthy Chinese Volunteers. *Ultrasound Med Biol* 43(5):1031–1039 [PubMed: 28283327]
12. Claudon M, Dietrich CF, Choi BI, et al. (2013) Guidelines and good clinical practice recommendations for contrast enhanced ultrasound (CEUS) in the liver—update 2012: a WFUMB-EFSUMB initiative in cooperation with representatives of AFSUMB, AIUM, ASUM, FLAUS and ICUS. *Ultrasound Med Biol* 39(2):187–210 [PubMed: 23137926]
13. Wilson SR, Greenbaum LD, Goldberg BB (2009) Contrast-enhanced ultrasound: what is the evidence and what are the obstacles? *Am J Roentgenol* 193(1):55–60 [PubMed: 19542395]
14. Wilson SR, Lyshchik A, Piscaglia F, et al. (2017) CEUS LI-RADS: algorithm, implementation, and key differences from CT/MRI. *Abdom Radiol* 43(1):1–16
15. Zarzour JG, Lockhart ME, West J, et al. (2017) Contrast-enhanced ultrasound classification of previously indeterminate renal lesions. *J Ultrasound Med* 36(9):1819–1827 [PubMed: 28429490]
16. Barr RG, Peterson C, Hindi A (2013) Evaluation of indeterminate renal masses with contrast-enhanced US: a diagnostic performance study. *Radiology* 271(1):133–142 [PubMed: 24475802]
17. Mauri G, Porazzi E, Cova L, et al. (2014) Intraprocedural contrast-enhanced ultrasound (CEUS) in liver percutaneous radiofrequency ablation: clinical impact and health technology assessment. *Insights Imaging* 5(2):209–216 [PubMed: 24563244]
18. Zhao X, Wang W, Zhang S, et al. (2012) Improved outcome of percutaneous radiofrequency ablation in renal cell carcinoma: a retrospective study of intraoperative contrast-enhanced ultrasonography in 73 patients. *Abdom Radiol* 37(5):885–891
19. Sever A, Jones S, Cox K, et al. (2009) Preoperative localization of sentinel lymph nodes using intradermal microbubbles and contrast-enhanced ultrasonography in patients with breast cancer. *Br J Surg* 96(11):1295–1299 [PubMed: 19847869]
20. Sparchez Z, Radu P, Zaharia T, et al. (2011) Usefulness of contrast enhanced ultrasound guidance in percutaneous biopsies of liver tumors. *J Gastrointest Liver Dis* 20(2):191–196

21. Wu W, Chen MH, Yan K, et al. (2006) Application of contrast-enhanced ultrasound to increase the diagnostic rate of liver tumor by biopsy. *Zhonghua yi xue za zhi* 86(2):116–120 [PubMed: 16620718]
22. Yoon SH, Lee KH, Kim SY, et al. (2010) Real-time contrast-enhanced ultrasound-guided biopsy of focal hepatic lesions not localized on B-mode ultrasound. *Eur Radiol* 20(8):2047–2056 [PubMed: 20309559]
23. Cao B- S, Wu J- H, Li X- L, et al. (2011) Sonographically guided transthoracic biopsy of peripheral lung and mediastinal lesions. *J Ultrasound Med* 30(11):1479–1490 [PubMed: 22039020]
24. Wang S, Yang W, Zhang H, et al. (2015) The role of contrast-enhanced ultrasound in selection indication and improving diagnosis for transthoracic biopsy in peripheral pulmonary and mediastinal lesions. *BioMed Res Int* 2015:1–8
25. Mao F, Dong Y, Ji Z, et al. (2017) Comparison of contrast-enhanced ultrasound and conventional ultrasound for guiding peripheral pulmonary biopsies. *Int J Clin Exp Med* 10(2):3677
26. Sugimoto M, Takagi T, Hikichi T, et al. (2015) Conventional versus contrast-enhanced harmonic endoscopic ultrasonography-guided fine-needle aspiration for diagnosis of solid pancreatic lesions: a prospective randomized trial. *Pancreatol* 15(5):538–541 [PubMed: 26145837]
27. Boczek J, Messing E, Dogra V (2006) Transrectal sonography in prostate evaluation. *Radiol Clin* 44(5):679–687
28. Halpern EJ, Gomella LG, Forsberg F, et al. (2012) Contrast enhanced transrectal ultrasound for the detection of prostate cancer: a randomized, double-blind trial of dutasteride pretreatment. *J Urol* 188(5):1739–1745 [PubMed: 22998915]
29. Kundavaram CR, Halpern EJ, Trabulsi EJ (2012) Value of contrast-enhanced ultrasonography in prostate cancer. *Curr Opin Urol* 22(4):303–309 [PubMed: 22617061]
30. Trabulsi EJ, Sackett D, Gomella LG, et al. (2010) Enhanced transrectal ultrasound modalities in the diagnosis of prostate cancer. *Urology* 76(5):1025–1033 [PubMed: 20719368]
31. van Hove A, Savoie P- H, Maurin C, et al. (2014) Comparison of image-guided targeted biopsies versus systematic randomized biopsies in the detection of prostate cancer: a systematic literature review of well-designed studies. *World J Urol* 32(4):847–858 [PubMed: 24919965]
32. Kuru TH, Fu`terer JJ, Schiffmann J, et al. (2015) Transrectal ultrasound (US), contrast-enhanced US, real-time elastography, HistoScanning, magnetic resonance imaging (MRI), and MRI-US fusion biopsy in the diagnosis of prostate cancer. *Eur Urol Focus* 1(2):117–126 [PubMed: 28723422]
33. Madsen HHT, Rasmussen F (2011) Contrast-enhanced ultrasound in oncology. *Cancer Imaging* 11(1A):S167 [PubMed: 22186152]
34. Huang DY, Yusuf GT, Daneshi M, et al. (2016) Contrast-enhanced US–guided interventions: improving success rate and avoiding complications using US contrast agents. *RadioGraphics* 37(2):652–664
35. Minami Y, Kudo M, Kawasaki T, et al. (2004) Treatment of hepatocellular carcinoma with percutaneous radiofrequency ablation: usefulness of contrast harmonic sonography for lesions poorly defined with B-mode sonography. *Am J Roentgenol* 183(1):153–156 [PubMed: 15208130]
36. Hocke M, Menges M, Topalidis T, et al. (2008) Contrast-enhanced endoscopic ultrasound in discrimination between benign and malignant mediastinal and abdominal lymph nodes. *J Cancer Res Clin Oncol* 134(4):473–480 [PubMed: 17891499]
37. Sever AR, Mills P, Jones SE, et al. (2011) Preoperative sentinel node identification with ultrasound using microbubbles in patients with breast cancer. *Am J Roentgenol* 196(2):251–256 [PubMed: 21257873]
38. Kono Y, Lucidarme O, Choi S- H, et al. (2007) Contrast-enhanced ultrasound as a predictor of treatment efficacy within 2 weeks after transarterial chemoembolization of hepatocellular carcinoma. *J Vasc Interv Radiol* 18(1):57–65 [PubMed: 17296705]
39. Shaw CM, Eisenbrey JR, Lyshchik A, et al. (2015) Contrast-enhanced ultrasound evaluation of residual blood flow to hepatocellular carcinoma after treatment with transarterial chemoembolization using drug-eluting beads. *J Ultrasound Med* 34(5):859–867 [PubMed: 25911704]

40. Iqbal SI, Stuart KE (2018) Assessment of tumor response in patients receiving systemic and nonsurgical locoregional treatment of hepatocellular cancer. In: Goldberg RM (ed) UpToDate. Waltham: UpToDate
41. Hines-Peralta A, Goldberg SN (2016) Radiofrequency ablation and cryoablation of renal cell carcinoma. In: Ross ME (ed) UpToDate. Waltham: UpToDate Inc
42. Barwari K, Wijkstra H, van Delden OM, et al. (2013) Contrast-Enhanced ultrasound for the evaluation of the cryolesion after laparoscopic renal cryoablation: an initial report. *J Endourol* 27(4):402–407 [PubMed: 23092215]
43. Sanz E, Hevia V, Arias F, et al. (2015) Contrast-enhanced ultrasound (CEUS): an excellent tool in the follow-up of small renal masses treated with cryoablation. *Curr Urol Rep* 16(1):1–5 [PubMed: 25604651]
44. Zeccolini G, Del Biondo D, Cicero C, et al. (2014) Comparison of contrast-enhanced ultrasound scan (CEUS) and MRI in the followup of cryoablation for small renal tumors. *Exp 25 Cases* . <https://doi.org/10.5301/RU.2014.11986>
45. Eisenbrey JR, Shaw CM, Lyshchik A, et al. (2015) Contrast-enhanced subharmonic and harmonic ultrasound of renal masses undergoing percutaneous cryoablation. *Acad Radiol* 22(7):820–826 [PubMed: 25882093]
46. Chen M- H, Yang W, Yan K, et al. (2004) Large liver tumors: protocol for radiofrequency ablation and its clinical application in 110 patients—mathematic model, overlapping mode, and electrode placement process. *Radiology* 232(1):260–271 [PubMed: 15166323]
47. Roccarina D, Garcovich M, Ainora ME, et al. (2015) Usefulness of contrast enhanced ultrasound in monitoring therapeutic response after hepatocellular carcinomatreatment. *World J Hepatol* 7(14): 1866 [PubMed: 26207168]
48. Du J, Li H- L, Zhai B, et al. (2015) Radiofrequency ablation for hepatocellular carcinoma: utility of conventional ultrasound and contrast-enhanced ultrasound in guiding and assessing early therapeutic response and short-term follow-up results. *Ultrasound Med Biol* 41(9):2400–2411 [PubMed: 26055968]
49. Hoeffel C, Pousset M, Timsit M- O, et al. (2010) Radiofrequency ablation of renal tumours: diagnostic accuracy of contrast-enhanced ultrasound for early detection of residual tumour. *Eur Radiol* 20(8):1812–1821 [PubMed: 20204642]
50. Dill-Macky MJ, Asch M, Burns P, et al. (2006) Radiofrequency ablation of hepatocellular carcinoma: predicting success using contrast-enhanced sonography. *Am J Roentgenol* 186(5):S287–S295 [PubMed: 16632690]
51. Hou X, Jin Z, Xu C, et al. (2015) Contrast-enhanced harmonic endoscopic ultrasound-guided fine-needle aspiration in the diagnosis of solid pancreatic lesions: a retrospective study. *PLoS ONE* 10(3):e0121236 [PubMed: 25793739]
52. Seicean A, Badea R, Moldovan-Pop A, et al. (2017) Harmonic contrast-enhanced endoscopic ultrasonography for the guidance of fine-needle aspiration in solid pancreatic masses. *Ultraschall in der Medizin-Eur J Ultrasound* 38(02):174–182
53. Frauscher F, Klauser A, Volgger H, et al. (2002) Comparison of contrast enhanced color Doppler targeted biopsy with conventional systematic biopsy: impact on prostate cancer detection. *J Urol* 167(4):1648–1652 [PubMed: 11912381]
54. Linden RA, Trabulsi EJ, Forsberg F, et al. (2007) Contrast enhanced ultrasound flash replenishment method for directed prostate biopsies. *J Urol* 178(6):2354–2358 [PubMed: 17936814]
55. Mitterberger MJ, Aigner F, Horninger W, et al. (2010) Comparative efficiency of contrast-enhanced colour Doppler ultrasound targeted versus systematic biopsy for prostate cancer detection. *Eur Radiol* 20(12):2791–2796 [PubMed: 20571801]
56. Taverna G, Morandi G, Seveso M, et al. (2011) Colour Doppler and microbubble contrast agent ultrasonography do not improve cancer detection rate in transrectal systematic prostate biopsy sampling. *BJU Int* 108(11):1723–1727 [PubMed: 21756276]
57. Zhao H- X, Xia C- X, Yin H- X, et al. (2013) The value and limitations of contrast-enhanced transrectal ultrasonography for the detection of prostate cancer. *Eur J Radiol* 82(11):e647

58. Meloni MF, Bertolotto M, Alberzoni C, et al. (2008) Follow-up after percutaneous radiofrequency ablation of renal cell carcinoma: contrast-enhanced sonography versus contrast-enhanced CT or MRI. *Am J Roentgenol* 191(4):1233–1238 [PubMed: 18806170]
59. Kong W- T, Zhang W- W, Guo H- Q, et al. (2011) Application of contrast-enhanced ultrasonography after radiofrequency ablation for renal cell carcinoma: is it sufficient for assessment of therapeutic response? *Abdom Imaging* 36(3):342–347 [PubMed: 21107560]
60. Li X, Liang P, Yu J, et al. (2013) Role of contrast-enhanced ultrasound in evaluating the efficiency of ultrasound guided percutaneous microwave ablation in patients with renal cell carcinoma. *Radiol Oncol* 47(4):398–404 [PubMed: 24294186]
61. Garbajs M, Popovic P (2016) Contrast-enhanced ultrasound for assessment of therapeutic response after percutaneous radiofrequency ablation of small renal tumors. *Age (years)* 77:58–94
62. Meloni MF, Goldberg SN, Livraghi T, et al. (2001) Hepatocellular carcinoma treated with radiofrequency ablation: comparison of pulse inversion contrast-enhanced harmonic sonography, contrast-enhanced power Doppler sonography, and helical CT. *Am J Roentgenol* 177(2):375–380 [PubMed: 11461867]
63. Choi D, Lim HK, Lee WJ, et al. (2003) Early assessment of the therapeutic response to radio frequency ablation for hepatocellular carcinoma. *J Ultrasound Med* 22(11):1163–1172 [PubMed: 14620886]
64. Wen YL, Kudo M, Zheng RQ, et al. (2003) Radiofrequency ablation of hepatocellular carcinoma: therapeutic response using contrast-enhanced coded phase-inversion harmonic sonography. *Am J Roentgenol* 181(1):57–63 [PubMed: 12818830]
65. Kim CK, Choi D, Lim HK, et al. (2005) Therapeutic response assessment of percutaneous radiofrequency ablation for hepatocellular carcinoma: utility of contrast-enhanced agent detection imaging. *Eur J Radiol* 56(1):66–73 [PubMed: 15913940]
66. Yu X- L, Li A- H, Jiang T- A, et al. (2007) Comparison of contrast enhanced ultrasound and contrast enhanced CT or MRI in monitoring percutaneous thermal ablation procedure in patients with hepatocellular carcinoma: a multi-center study in China. *Ultrasound Med Biol* 33(11):1736–1749 [PubMed: 17629608]
67. Salvaggio G, Campisi A, Greco VL, et al. (2010) Evaluation of posttreatment response of hepatocellular carcinoma: comparison of ultrasonography with second-generation ultrasound contrast agent and multidetector CT. *Abdom Imaging* 35(4):447–453 [PubMed: 19562414]
68. Bo X- W, Xu H- X, Sun L- P, et al. (2014) Bipolar radiofrequency ablation for liver tumors: comparison of contrast-enhanced ultrasound with contrast-enhanced MRI/CT in the posttreatment imaging evaluation. *Int J Clin Exp Pathol* 7(9):6108 [PubMed: 25337258]
69. Minami Y, Kudo M, Kawasaki T, et al. (2003) Transcatheter arterial chemoembolization of hepatocellular carcinoma: usefulness of coded phase-inversion harmonic sonography. *Am J Roentgenol* 180(3):703–708 [PubMed: 12591679]
70. Kim HJ, Kim TK, Kim PN, et al. (2006) Assessment of the therapeutic response of hepatocellular carcinoma treated with transcatheter arterial chemoembolization. *J Ultrasound Med* 25(4):477–486 [PubMed: 16567437]
71. Xia Y, Kudo M, Minami Y, et al. (2008) Response evaluation of transcatheter arterial chemoembolization in hepatocellular carcinomas: the usefulness of sonazoid-enhanced harmonic sonography. *Oncology* 75(1):99–105 [PubMed: 19092278]
72. Morimoto M, Shirato K, Sugimori K, et al. (2003) Contrast-enhanced harmonic gray-scale sonographic–histologic correlation of the therapeutic effects of transcatheter arterial chemoembolization in patients with hepatocellular carcinoma. *Am J Roentgenol* 181(1):65–69 [PubMed: 12818831]
73. Liu M, Lin M- X, Xu Z- F, et al. (2015) Comparison of contrast-enhanced ultrasound and contrast-enhanced computed tomography in evaluating the treatment response to transcatheter arterial chemoembolization of hepatocellular carcinoma using modified RECIST. *Eur Radiol* 25(8):2502–2511 [PubMed: 25702094]

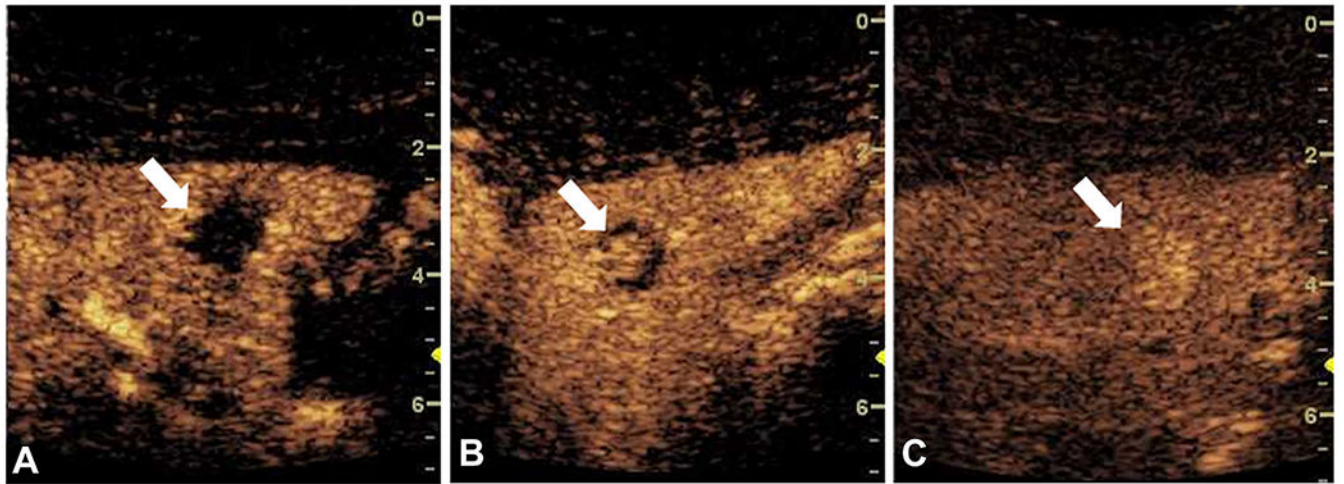


Fig. 1. Contrast-enhanced ultrasound of an indeterminate liver lesion (arrow) showing peripheral discontinuous globular enhancement (from the left of the image and extending towards the center of the lesion) with progressive central filling and persistent hyper-enhancement, consistent with hemangioma. **(A)** 16 s after bolus injection. **(B)** 39 s after bolus injection. **(C)** 167 s after bolus injection.

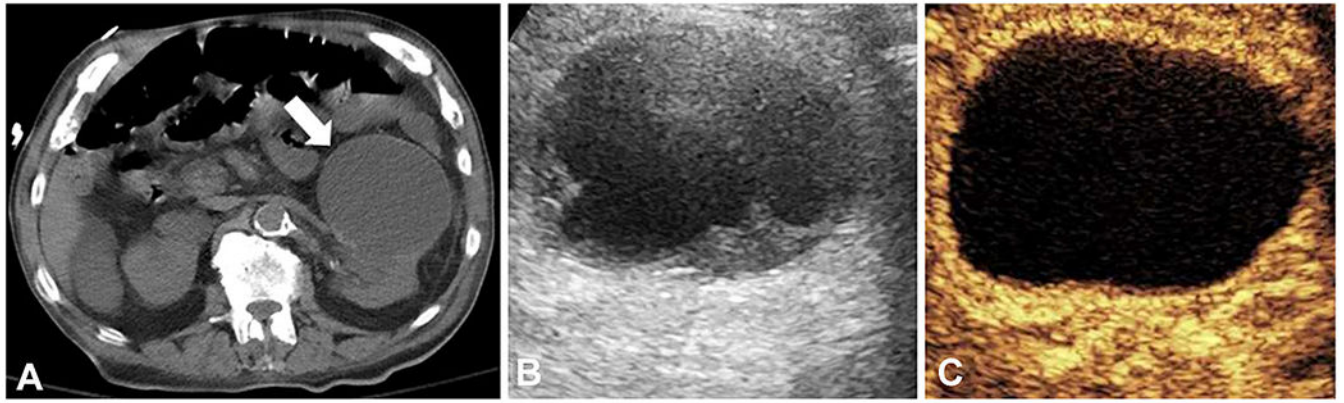


Fig. 2. Indeterminate renal lesion better characterized by contrast-enhanced ultrasound. **(A)** Non-contrast CT demonstrating a $7.4 \times 4.2 \times 8.6$ cm exophytic left renal mass (arrow). **(B)** Gray-scale ultrasound demonstrating a $7.1 \times 7.0 \times 6.2$ complex hypoechoic cystic lesion with septations. **(C)** Contrast-enhanced ultrasound demonstrating a $7.1 \times 7.0 \times 6.2$ complex cystic lesion with no internal enhancement consistent with a benign or indolent lesion.

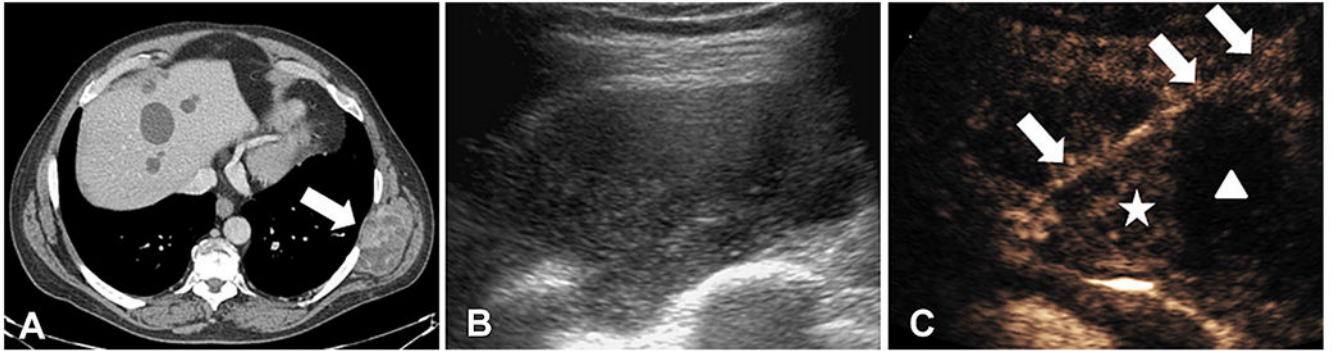


Fig. 3. Contrast-enhanced biopsy guidance. **(A)** Contrast-enhanced CT scan showing an enlarging $8 \times 4 \times 5$ cm left flank mass (arrow) in the setting of known stable metastatic melanoma. **(B)** Gray-scale ultrasound demonstrating a $8 \times 4 \times 5$ cm complex hypoechoic lesion. **(C)** Contrast-enhanced ultrasound of the same lesion showing clear areas of perfusion (star) and lack of perfusion. The biopsy needle is depicted (arrow), passing through an area of perfused lesion (star). Areas of poor enhancement (triangle) represent hypo-perfused or necrotic regions of the lesion that may be less likely to provide a definitive diagnosis.

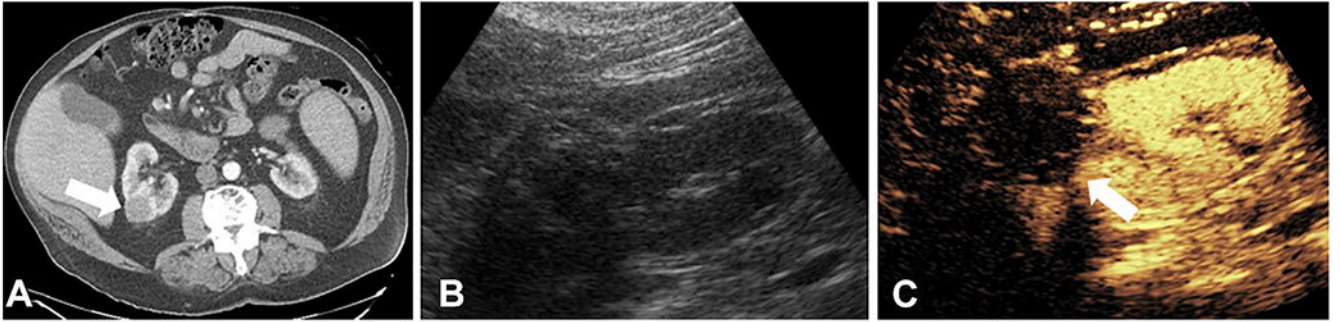


Fig. 4. Treatment effect monitoring by contrast-enhanced ultrasound after cryoablation of high-risk renal lesion. **(A)** 3.4-cm right renal lesion (arrow) with soft tissue enhancement concerning for renal cell carcinoma. **(B)** Gray-scale ultrasound of treated kidney. **(C)** Contrast-enhanced ultrasound of the same window showing treatment ablation cavity without nodular enhancement. Minimal peripheral enhancement suggestive of post-procedure scar. No viable tumor is present.

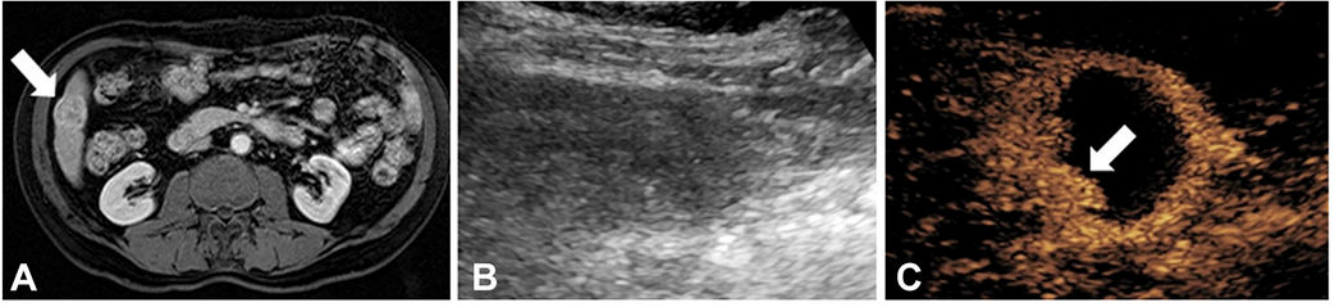


Fig. 5. Treatment effect monitoring by contrast-enhanced ultrasound after trans-arterial chemoembolization (TACE) of hepatocellular carcinoma. **(A)** Post-contrast T1-weighted fat suppressed MRI demonstrating a $2.8 \times 2.6 \times 2.5$ cm segment VI LI-RADS 5 lesion (arrow) with arterial phase enhancement (and washout on delayed imaging) before TACE treatment. **(B)** Gray-scale ultrasound with difficulty delineating the lesion bed post-treatment. **(C)** Contrast-enhanced ultrasound of the same ultrasound window demonstrating the lesion with partial treatment response and some residual enhancement (arrow) concerning for viable tumor.

Table 1.

Patterns of CEUS of focal liver lesions [3]

Lesion	Arterial phase (up to 45 s)	Portal phase (45–120 s)	Late venous phase (Beyond 120 s)
Simple cyst	Non-enhancing	Non-enhancing	Non-enhancing
Hemangioma	Peripheral enhancement	Centripetal filling or peripheral globular enhancement	Hyper-enhancement
Focal nodular hyperplasia	Central enhancement	Hyper-enhancement with central scar	Iso-/hyper-enhancement
Hepatic adenoma	Variable enhancement	Variable enhancement	Variable vs. hypo-enhancement
Hepatocellular carcinoma	Hyper-enhancement	Iso-/non-enhancement	Hypo-/non-enhancement
Cholangiocarcinoma	Rim enhancement	Hypo-enhancement	Non-enhancement
Metastatic lesion	Rapid hyper-enhancement (hyper-vascular) or rim enhancement (hypo-vascular)	Iso-/non-enhancement	Hypo-/non-enhancement

Table 2.
Impact of CEUS guidance on sensitivity or diagnostic accuracy of solid organ tissue biopsy

Study	N: CEUS vs. routine	Solid lesion	CEUS-guided sensitivity* or diagnostic accuracy (%) ^d	Routine sensitivity* or diagnostic accuracy (%) ^a	P value
Wu et al. [21]	149 vs. 153	Hepatic	96.0 [*]	87.6 [*]	$P = 0.0165^*$
Sparchez et al. [20]	18 vs. 30	Hepatic	100 ^d	86.6 ^d	$P < 0.05^d$
Hou et al. [51]	58 vs. 105	Pancreas	81.6 [*]	70.8 [*]	$P = 0.88^*$
Seicean et al. [52]	51 vs. Internal Control	Pancreas	86.5 ^d	78.4 ^d	$P = 0.35^d$
Cao et al. [23]	62 vs. 59	Pulmonary	93.6 ^d	78.0 ^d	$P < 0.05^d$
Wang et al. [24]	82 vs. 60	Pulmonary	96.3 ^d	80 ^d	$P = 0.002^d$
Mao et al. [25]	121 vs. 131	Pulmonary	95.9 ^d	87.0 ^d	$P = 0.013^d$

* Study reported sensitivity

^d Study reported diagnostic accuracy

Table 3.

Impact of CEUS guidance on detection rate of transrectal prostate biopsy

Study	N: CEUS vs. routine (per core)*	CEUS detection rate (per core)	Routine detection rate (per core)	P value (per core)
Frauscher et al. [31, 53]	230 vs. internal control (1139 vs. 2300)	24.4% (10.4%)	22.6% (5.3%)	$P = 0.58$ ($P < 0.0001$)
Linden et al. [31, 54]	60 vs. internal control (225 vs. 600)	22% (13%)	27% (8.3%)	$P > 0.25$ ($P = 0.034$)
Mitterberger et al. [31, 55]	1776 vs. internal control (8880 vs. 17,760)	27% (10.8%)	23% (5.1%)	$P < 0.0001$ ($P < 0.0001$)
Taverna et al. [31, 56]	100 vs. 100	29%	31%	$P = 0.3$
Halpern et al. [28, 31]	272 vs. internal control (1237 vs. 3264)	26% (16.4%)	39% (8.5%)	$P < 0.0001$ ($P < 0.0001$)
Zhao et al. [31, 57]	65 vs. internal control (44 vs. 336) ^a	35.4% (75%) ^a	41.5% (48.2%) ^a	Not reported ($P = 0.0001$) ^a

* In select studies (indicated by separate analyses in parenthesis), statistical analysis was also performed per tissue core retrieved in addition to per patient to assess if CEUS had a higher detection yield per core compared with routine technique

^a Per core analysis was limited to the 28 patients in which an abnormality was noted on CEUS

Table 4.

Performance of modern CEUS on assessment of tumor response after ablative therapy

Study	N	Ablation*	Lesion	CEUS sensitivity to incomplete treatment (timing) ^a	CEUS specificity to incomplete treatment (timing) ^a	Reference standard
Meloni et al. [58]	28	RFA	Renal	96.6% (variable-beginning at 4 months)	100% (variable-beginning at 4 months)	CT/MRI performed at same time as CEUS
Hoefel et al. [49]	66	RFA	Renal	64% (< 24 h) 79% (6 weeks)	98% (< 24 h) 100% (6 weeks)	CT/MRI 12 months after ablation
Kong et al. [59]	64	RFA	Renal	100% (1 month)	96.6% (1 month)	CT 1 month after ablation
Li et al. [60]	83	MWA	Renal	100% (3 days)	97.1% (3 days)	CT/MRI 3 days after ablation
Barwari et al. [42]	45	CA	Renal	Not reported	92% (3 months) 90% (12 months)	CT/MRI performed at same time as CEUS
Zeccolini et al. [44]	25	CA	Renal	100% (every 3 months first year, every 6 months after)	100% (every 3 months first year, every 6 months after)	MRI performed at same time as CEUS
Sanz et al. [43]	16	CA	Renal	100% (3 months, every 6 months after)	96.2% (3 months, every 6 months after)	CT 3 months after ablation, every 6 months after
Garbajs et al. [61]	14	RFA	Renal	100% (1 week after CT)	100% (1 week after CT)	CT variable time after ablation
Meloni et al. [62]	43	RFA	Hepatic	83.3% (4 months)	100% (4 months)	CT 4 months after ablation
Choi et al. [63]	81	RFA	Hepatic	100% (< 24 h)	100% (< 24 h)	CT 1 month after ablation
Wen et al. [64]	91	RFA	Hepatic	95.3% (5–7 days)	100% (5–7 days)	CT 5–7 days after ablation
Kim et al. [65]	97	RFA	Hepatic	Not reported	99% (< 24 h)	CT 1 month after ablation
Dill-Macky et al. [50]	21	RFA	Hepatic	40% (15–60 min) 83% (2–4 weeks)	94% (15–60 min) 94% (2–4 weeks)	CT or MRI 2–4 weeks after ablation
Yu et al. [66]	139	RFA	Hepatic	97% (1 month)	98.2% (1 month)	CT/MRI 1 month after ablation
Salvaggio et al. [67]	110	RFA	Hepatic	83.3% (< 24 h)	100% (< 24 h)	CT 1 month after ablation
Bo et al. [68]	73	RFA	Hepatic	87.5% (1 month)	96.9% (1 month)	CT/MRI 1 month after ablation
Du et al. [48]	78	RFA	Hepatic	60% (30 min)	100% (30 min)	MRI 1 month after ablation

* RFA radiofrequency ablation, MWA microwave ablation, CA cryoablation

^aTime after ablative therapy at which CEUS examination was performed

Performance of CEUS on assessing hepatic tumor response after intra-arterial chemoembolization therapy

Table 5.

Study	N	CEUS sensitivity (interval)*	CEUS specificity (interval)*	Reference standard
Kono et al. [38]	23	100% (< 2 weeks)	83.3% (< 2 weeks)	CT/MRI 6 months after treatment or biopsy or angiography
Minami et al. [69]	44	100% (< 1 week)	100% (< 1 week)	CT 2 months after treatment
Kim et al. [70]	29	93% (variable)	65% (variable)	Angiography at a variable time after treatment
Xia et al. [71]	43	100% (1 week)	69% (1 week)	CT 1 week after treatment
Morimoto et al. [72]	29	100% (1 week)	81% (1 week)	Biopsy 7 days after treatment
Salvaggio et al. [67]	38	100% (< 24 h)	100% (< 24 h)	CT 1 month after treatment or angiography
Liu et al. [73]	130	95.9% (2–12 weeks)	100% (2–12 weeks)	Angiography or biopsy at a variable time after treatment
Shaw et al. [39]	14	100% (1–2 weeks)	100% (1–2 weeks)	CT/MRI 1 month after treatment

* Time after ablative therapy at which CEUS examination was performed